Available online at www.sciencedirect.com
ScienceDirect
Journal of the Nigerian Mathematical Society 34 (2015) 169–180
Journal of the Nigerian Mathematical Society
www.elsevier.com/locate/jnnms

Radiation, inclined magnetic field and cross-diffusion effects on flow over a stretching surface

C.S.K. Raju[a], N. Sandeep[b,*], C. Sulochana[b], V. Sugunamma[c], M. Jayachandra Babu[a]

[a] *Fluid Dynamics Division, VIT University, Vellore-632014, India*
[b] *Department of Mathematics, Gulbarga University, Gulbarga-585106, India*
[c] *Department of Mathematics, S.V. University, Tirupati-517502, India*

Received 26 December 2014; received in revised form 18 February 2015; accepted 21 February 2015
Available online 4 April 2015

Abstract

The steady two-dimensional flow over a vertical stretching surface in presence of aligned magnetic field, cross-diffusion and radiation effects are considered. The governing partial differential equations are transformed to nonlinear ordinary differential equation by using similarity transformation and then solved numerically by using bvp4c with MATLAB package. The effects of various non-dimensional governing parameters on velocity, temperature, concentration profiles along friction factor, Nusselt and Sherwood numbers are discussed and presented through graphs and tables'.We observed that increase in aligned angle strengthen the magnetic field and decreases the velocity profile of the flow and enhances the heat transfer rate. Comparisons with existed results are presented.

Keywords: Stretching sheet; Aligned magnetic field; Cross diffusion; Radiation; Convection

1. Introduction

In recent years convective heat and mass transfer over a stretching sheet plays major role because of it tremendous applications in engineering and sciences. For this reason now a day's large amount of work is focused in this area. Prasad et al. [1] have given detailed description about the effects of different physical properties of fluids on MHD flow. A steady two dimensional MHD flow analysis in presence of radiation by using homotopy analysis method was discussed by Rashidi et al. [2]. Boundary layer flow through exponentially stretching sheet in the presence of stratified medium by using Shooting technique was discussed by Swathy Mukhopadhyay [3]. Pavithra and Gireesha [4] used Runge–Kutta method and analysed radiation effect on dusty fluid over exponentially stretching sheet. Zaimi et al. [5] analyzed steady two dimensional flow of a nanofluid over a stretching/shrinking sheet. Wang and Mujumdar [6] given good literature on heat transfer characteristics of nanofluids.

Peer review under responsibility of Nigerian Mathematical Society.
* Corresponding author.
E-mail address: nsreddy.dr@gmail.com (N. Sandeep).

http://dx.doi.org/10.1016/j.jnnms.2015.02.003

Rana and Bhargava [7] used finite element and finite difference methods for nonlinear stretching sheet problem. Zaimi et al. [8] extended the work of Rana and Bhargava and studied heat transfer and boundary layer flow of a nano fluid over a stretching/shrinking sheet. Radiation effect on MHD viscous fluid over exponentially stretching sheet in porous medium was analyzed by Ahmad et al. [9]. Hady et al. [10] studied heat transfer characteristics of nonlinear stretching sheet in the presence of thermal radiation. The boundary layer flow of a stagnation point over a stretching sheet was analysed by Bhattacharya [11]. He found that the rate of heat transfer enhances due to its unsteadiness and he compared the unique solution to dual solution. Free convection heat transfer through a horizontal plate with soret and dufour effect was discussed by Lakshminarayana and Murthy [12]. Ece [13] proposed the similarity analysis for the laminar free convection boundary layer flow in the presence of a transverse magnetic field. Hamad and Ferdows [14]. The thermal conductivity of solid particles is several times more than that of the base or convectional fluids was discussed by Das et al. [15] in the book nanofluids science and technology. In this book they clearly explained the thermal properties and behavior of the particles at different temperatures. Boungiorno [16] presented different theories on enhanced heat transfer characteristics of nanofluids and he concluded that thermal dispersion phenomenon cannot explain fully about the high heat transfer coefficients in nanofluids. A clear investigation on nanofluid thermal properties was done by Phillip et al. [17]. Radiation effects on unsteady MHD flow over moving vertical plate was studied by Mohan Krishna et al. [18]. The researchers [19–21] have been given their valuable contribution to analyze the heat transfer characteristics in convective flows. All the above studies focused on transverse magneticfield with radition. Khidir and Sibanda [22] considered cross-diffusion effects for a steady flow over an exponentially stretching surface. Makinde and Ogulu [23] analyzed thermal radiation and transverse magneticfield effects on a flow over a vertical porous plate. Makinde [24] discussed mixed convection flow over a vertical porous plate by considering radiation and chemical reaction effects. The researchers Seini and Makinde [25] studied MHD boundary layer flow towards exponentially stretching surface. Shateyi and Makinde [26] presented MHD stagnation point flow over a radially heated stretched disk.

To the author's knowledge no studies have been reported on effects of aligned magnetic field, cross-diffusion and radiation on steady two-dimensional flow over a vertical stretching surface. The governing partial differential equations are transformed to nonlinear ordinary differential equation by using similarity transformation and then solved by numerically by using bvp4c with MATLAB package. The effects of various non-dimensional parameters on velocity, temperature, concentration profiles are discussed and presented through graphs. Also the effect of physical parameters on friction factor, Nusselt and Sherwood numbers are analyzed and presented through tables.

2. Flow analysis

Consider a steady, two dimensional, laminar, incompressible and electrically conducting boundary layer flow over a permeable stretching sheet, where the sheet is along y direction. A non uniform aligned magneticfield $B(x) = B_0 x^{1/3}$ is applied to the flow. Aligned magneticfield with acute angle gama (γ) applying along y direction. At $\gamma = \pi/2$ this magneticfield acts like transverse magneticfield (because $\sin(\pi/2) = 1$). A uniform stretching velocity $u_x(x) = cx^{1/3}$ is considered, where c is constant. The convective heat transfer is taken in to account. The boundary layer equations that governs the present flow subject to the Boussinesq approximations can be expressed as

$$\frac{\partial u}{\partial x} + \frac{\partial u}{\partial y} = 0 \tag{1}$$

$$u\frac{\partial u}{\partial x} + v\frac{\partial u}{\partial y} = \upsilon\frac{\partial^2 u}{\partial y^2} + g\beta_T(T - T_\infty) + g\beta_c(C - C_\infty) - \frac{\sigma B^2(x)}{\rho}\sin^2(\gamma)u \tag{2}$$

$$u\frac{\partial T}{\partial x} + v\frac{\partial T}{\partial y} = \alpha\frac{\partial^2 T}{\partial y^2} - \frac{1}{\rho c_p}\frac{\partial q_r}{\partial y} + \frac{D_m k_T}{c_s c_p}\frac{\partial^2 C}{\partial y^2} \tag{3}$$

$$u\frac{\partial C}{\partial x} + v\frac{\partial C}{\partial y} = D_m\frac{\partial^2 C}{\partial y^2} + \frac{D_m k_T}{c_s c_p}\frac{\partial^2 T}{\partial y^2} \tag{4}$$

where u and v are the velocity components in the directions of x and y respectively, υ is the kinematic viscosity, ρ is the fluid density, σ is the electrical conductivity, g is the acceleration due to gravity, β_T is the coefficient of Thermal expansion, β_c is the coefficient of volumetric expansion, α is the thermal conductivity, c_p is specific heat

capacitance, q_r is the radiative heat flux, c_s is the concentration susceptibility. D_m is the mass diffusivity, K_T is the thermal diffusion ratio, T_m is the mean fluid temperature.

By using Roseland approximation, the radiative heat flux q_r is given by

$$q_r = -\frac{4\sigma^*}{3k^*}\frac{\partial T^4}{\partial y} \tag{5}$$

where σ^* is the Steffen Boltzmann constant and k^* is the mean absorption coefficient. Considering the temperature differences within the flow sufficiently small such that T^4 may be expressed as the linear function of temperature. Then expanding T^4 in Taylor series about T_∞ and neglecting higher-order terms takes the form

$$T^4 \cong 4T_\infty^3 T - 3T_\infty^4. \tag{6}$$

In view of Eqs. (5) and (6), Eq. (3) reduces to

$$u\frac{\partial T}{\partial x} + v\frac{\partial T}{\partial y} = \alpha\frac{\partial^2 T}{\partial y^2} + \frac{16\sigma^* T_\infty^3}{3\rho c_p k^*}\frac{\partial^2 T}{\partial y^2} + \frac{D_m k_T}{c_s c_p}\frac{\partial^2 C}{\partial y^2}. \tag{7}$$

The corresponding boundary conditions are as follows

$$\begin{aligned} &u = u_w(x), \qquad v = v_w, \qquad -k\frac{dT}{dy} = h_f(x)(T_w - T), \qquad C_w = C_\infty + bx, \quad \text{at } y = 0, \\ &u \to 0, \qquad T \to T_\infty, \qquad C \to C_\infty, \quad \text{as } y \to \infty. \end{aligned} \tag{8}$$

The similarity solutions of Eqs. (2)–(4) subject to the boundary conditions (8) by introducing the following similarity transforms

$$\begin{aligned} &\eta = y\sqrt{c/\upsilon}x^{-1/3}, \qquad u = cx^{1/3}f'(\eta), \qquad v = \frac{1}{3}\left[cyx^{-2/3}f'(\eta) - 2\upsilon\eta f(\eta)\right] \\ &\theta(\eta) = \frac{T - T_\infty}{T_w - T_\infty}, \qquad \phi(\eta) = \frac{C - C_\infty}{C_w - C_\infty}. \end{aligned} \tag{9}$$

Substituting Eq. (9) into Eqs. (2), (4) and (7), where Eq. (1) is identically satisfied, we obtain the following ordinary differential equations:

$$f''' + \frac{2}{3}ff'' - \frac{1}{3}f'^2 + (\tau_T\theta + \tau_C\phi) - M\sin^2(\gamma)f' = 0 \tag{10}$$

$$(1 + R)\theta'' + \frac{2}{3}\Pr f\theta' + D_f \Pr\phi'' = 0 \tag{11}$$

$$\phi'' + \frac{2}{3}Scf\phi' + SrSc\theta'' = 0 \tag{12}$$

where prime denotes the derivative with respect to η, $M = \frac{\sigma B_0^2}{\rho c}$ is the magnetic field parameter, $\tau_T = \frac{g\beta_T(T_w - T_\infty)x^{1/3}}{c^2}$ is the thermal Buoyancy parameter, $\tau_C = \frac{g\beta_c(C_w - C_\infty)x^{1/3}}{c^2}$ is the concentration Buoyancy parameter, $D_f = \frac{D_m k_T(C_w - C_\infty)}{c_s c_p(T_w - T_\infty)}$ is the Dufour number, $Sr = \frac{D_m k_T(T_w - T_\infty)}{T_m\upsilon(C_w - C_\infty)}$ is the Soret number, $R = \frac{16\sigma^* T_\infty^3}{3kk^*}$ is the radiation parameter, $\Pr = \frac{\upsilon}{\alpha}$ is the Prandtl number and $Sc = \upsilon/D_m$ is the Schmidt number. The corresponding to the boundary conditions are as follows

$$\begin{aligned} &f(\eta) = f_w, \qquad f'(\eta) = 1, \qquad \theta'(\eta) = -Bi[1 - \theta(0)], \qquad \phi(\eta) = 1, \quad \text{at } \eta = 0, \\ &f(\eta) = 0, \qquad \theta(\eta) = 0, \qquad \phi(\eta) = 0, \quad \eta \to \infty \end{aligned} \tag{13}$$

where $f_w = -3v_w x^{1/3}/2\sqrt{c\upsilon}$ is the suction/injection parameter ($f_w > 0$ for suction and $f_w < 0$ injection) and $Bi = \frac{x^{1/3}h_f}{k}\sqrt{\frac{\upsilon}{c}}$ is the Biot number [23]. For engineering interest we computed friction factor $f''(0)$, rate of heat transfer $-\theta'(0)$ and mass transfer $\phi'(0)$ and discussed through table.

3. Results and discussion

The system of nonlinear ordinary differential equations (10)–(12) with the boundary conditions (13) are solved numerically using bvp4c with MATLAB package. The results obtained shows the influences of the non dimensional governing parameters, namely thermal radiation parameter R, Aligned angle γ, Soret number Sr, Dufour number D_f, Buoyancy parameters τ_T and τ_C and on velocity, temperature, concentration, skin friction, local Nusselt and Sherwood numbers are thoroughly investigated for suction/injection cases separately and presented through graphs and tables. In this study for numerical results we used $\Pr = 0.71, Sc = 0.6, \tau_T = \tau_C = 1, \gamma = \pi/3, M = 3, R = 1, Sr = 0.2, D_f = 0.3, Bi = 0.4$. These values kept as common in entire study except for the varied values as displayed in figures and tables.

Fig. 1 shows the effect of aligned angle on velocity profiles. It is clear from figure that increase in aligned angle decreases the velocity profiles of the fluid for both suction and injection cases. The reason behind this is increase in aligned angle causes to strengthen the magneticfield. Due to enhanced magneticfield, it generates opposite force to the flow, is called Lorentz force. This force declines the velocity boundary layer thickness. Fig. 2 displays the effect of Soret number on velocity profiles of the flow. It is evident from figure that increase in Soret number causes the increase in velocity profiles of the fluid and this effect is high on injection case compared to suction case. It is due to the fact that increase in Soret number decreases the boundary layer thickness of velocity profiles. Fig. 3 depicts the effect of Dufour number on velocity profiles of the flow. It is observed from figure that increase in Dufour number decreases the velocity profiles of the fluid and this effect is high on suction case compared to injection case. Generally increase in Dufour enhances the concentration of the fluid, which is indirectly helps to reduce the velocity field.

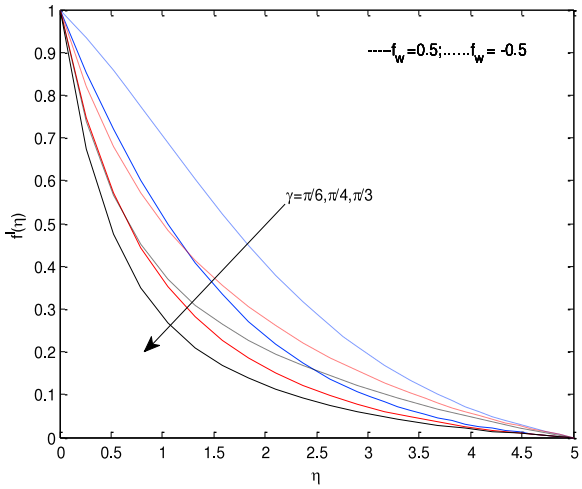

Fig. 1. Velocity profiles for different values of aligned angle γ.

Fig. 4 represents the effect of thermal Buoyancy parameter on velocity profiles. It is evident from figure that increase in thermal Buoyancy parameter causes the increase the velocity profiles of the fluid for both suction and injection cases. It may happen due to the reason that increasing the thermal buoyancy means there exists temperature difference in the flow which causes to reduce the thermal boundary layer and helps to enhance the fluid velocity. Similar type of results we observed from concentration Buoyancy parameter. Fig. 5 illustrates the effect of radiation parameter on velocity profiles. It is clear from figure that increase in thermal radiation parameter increases the velocity profiles of the fluid for both suction and injection cases. It agrees the general fact that increase in thermal radiation releases the heat energy to the flow and this helps to enhance the velocity profiles of the fluid. Fig. 6 shows the effect of Biot number on velocity profiles. It is observed from figure that increase in Biot number parameter increases the velocity profiles of the fluid for both suction and injection cases. It is due to the fact that Biot number enhances the heat transfer rate in solid body due to this reason velocity boundary layer become thinner.

Fig. 7 displays the effect of aligned angle on temperature profiles. It is evident from figure that increases in aligned angle increases the temperature profiles of the fluid for both suction and injection cases. It is due to the fact that a raise in magneticfiled parameter enhances the thermal and concentration boundary layer thickness. Fig. 8 illustrates

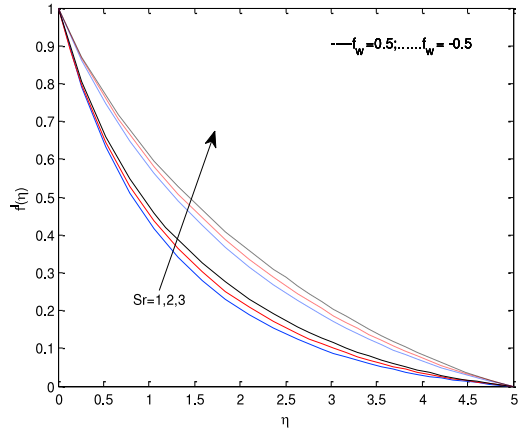

Fig. 2. Velocity profiles for different values of soret number Sr.

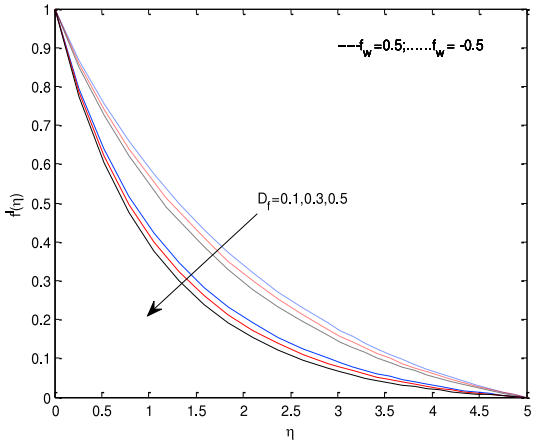

Fig. 3. Velocity profiles for different values of Dufour number D_f.

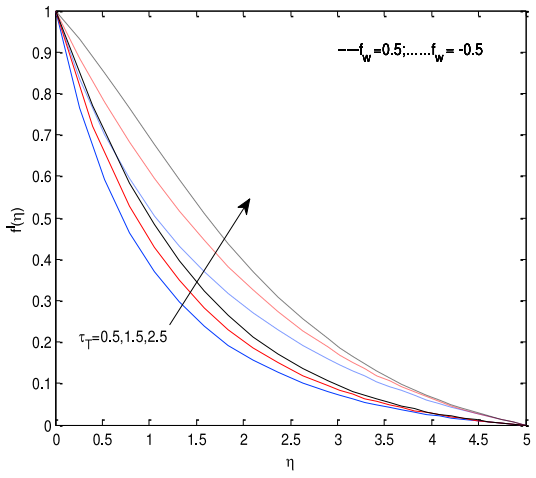

Fig. 4. Velocity profiles for different values of thermal buoyancy parameter τ_T.

the effect of soret number on temperature profiles. It is evident from figure that increase in soret parameter initially increases the temperature profiles of the fluid for both suction and injection cases. But at $\eta = 1.5$ level it takes reverse

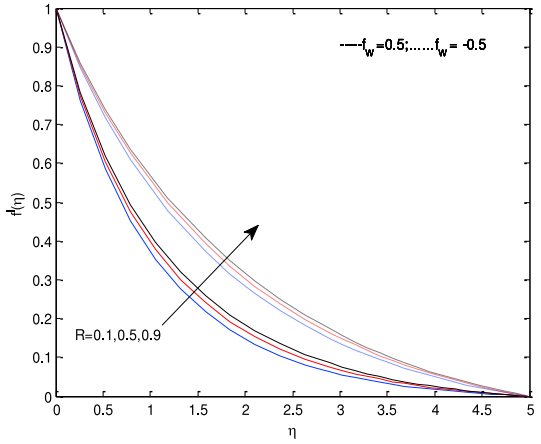

Fig. 5. Velocity profiles for different values of radiation parameter R.

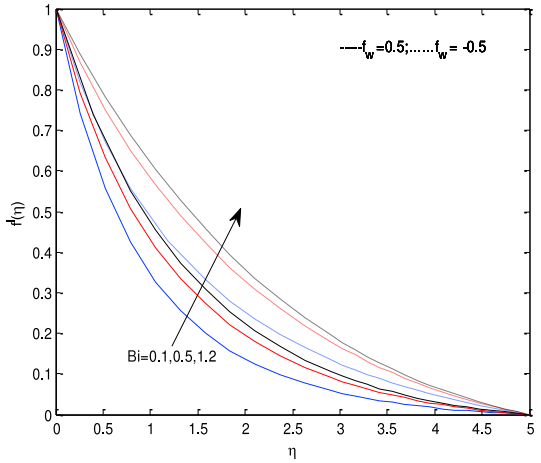

Fig. 6. Velocity profiles for different values of Biot number Bi.

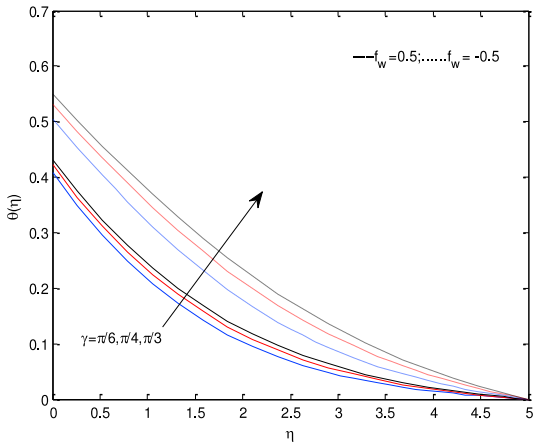

Fig. 7. Temperature profiles for different values of aligned angle γ.

action. This may happen due the domination property of absorption coefficient. A fall in temperature profiles by increase in Dufour number has seen from Fig. 9. Generally increase in Dufour number increases the thermal boundary

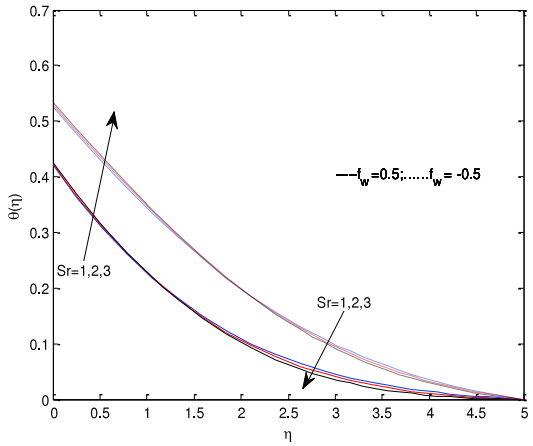

Fig. 8. Temperature profiles for different values of soret number Sr.

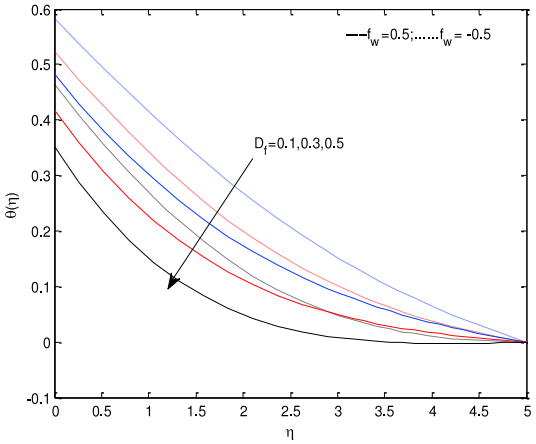

Fig. 9. Temperature profiles for different values of Dufour number D_f.

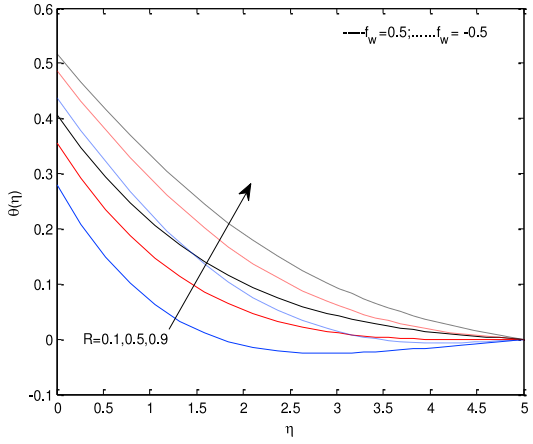

Fig. 10. Temperature profiles for different values of radiation parameter R.

layer. Fig. 10 illustrates the effect of radiation parameter on temperature profiles. It is observed from figures that increase in radiation parameter increases the temperature profiles of the fluid for both suction and injection cases. It is due to the general fact that increase in radiation parameter releases the heat energy to the flow, it helps to enhance the

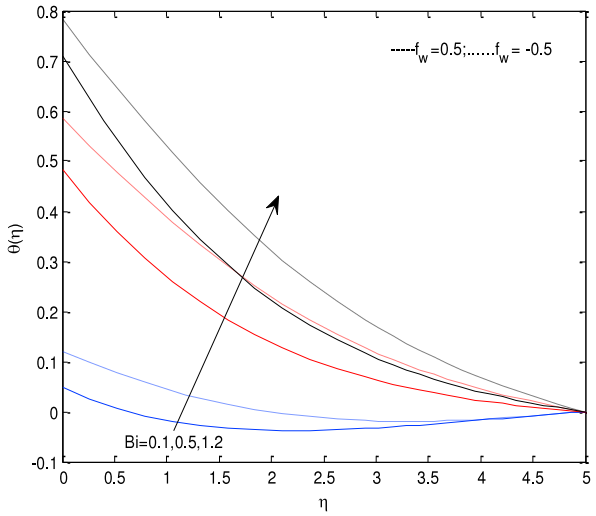

Fig. 11. Temperature profiles for different values of Biot number *Bi*.

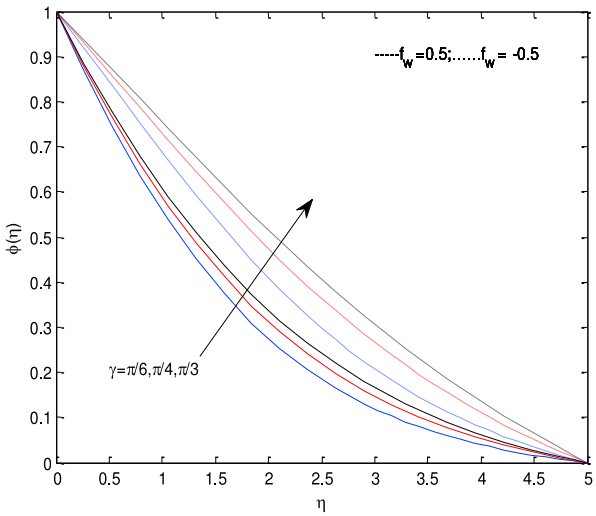

Fig. 12. Concentration profiles for different values of aligned angle γ.

temperature profiles. The similar type of results observed from Fig. 11. Here increase in Biot number increases the internal heat in solid surface, it helps to enhance the temperature profiles of the fluid.

Figs. 12–14 represents the effect of aligned angle, Soret and Dufour numbers, respectively on concentration profiles. It is evident from figures that increase in aligned angle, Soret and Dufour numbers increases the concentration profiles of the fluid for both suction and injection cases. These parameters help to reduce the concentration boundary layer thickness. But radiation parameter and Biot number shows reverse action on concentration profiles as displayed in Figs. 15 and 16 for both suction and injection cases.

Table 1 displays the comparison of the present values with existed results. Our results have excellent agreement with existed results of Cortell [27], Ferdows et al. [28] and Rashidi et al. [2]. Table 2 shows the effect of non dimensional parameters on friction factor, Nusselt number and Sherwood number. It is clear from table that increase in aligned angle reduces the friction factor, Sherwood number and increases the heat transfer rate for both suction and injection cases. Similar type of results observed for Dufour number. Increase in soret number increases the friction factor and decreases the rate of heat and mass transfer for both suction and injection cases. Increase in radiation parameter

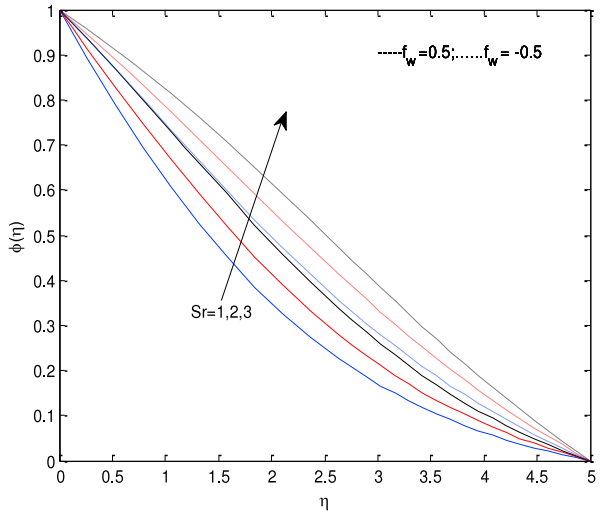

Fig. 13. Concentration profiles for different values of soret number *Sr*.

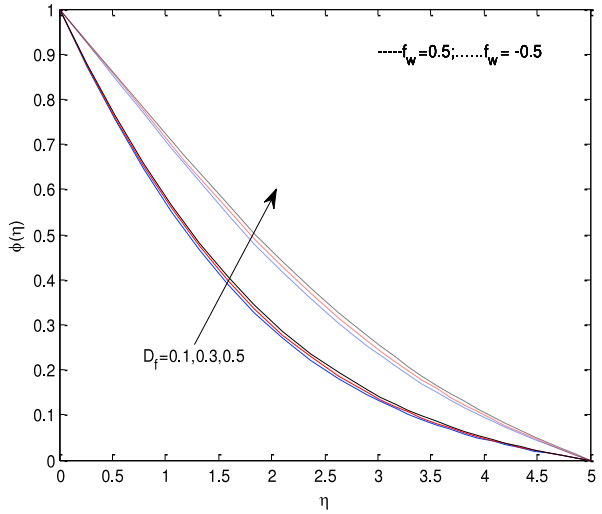

Fig. 14. Concentration profiles for different values of Dufour number D_f.

Table 1
Comparison of the values of $-\theta'(0)$ with published data when Pr $= 2$ and $Bi \to \infty$.

f_w	R	Cortell [27]	Ferdows et al. [28]	Rashidi et al. [2]	Present results
−0.5	4/3	0.2873762	0.287483	0.2877089	0.2877091
−0.5	0	0.3989462	0.398951	0.3990842	0.3990842
0	4/3	0.4430879	0.443323	0.4434039	0.4434040
0	0	0.7643554	0.764374	0.7643525	0.7643527
0.5	4/3	0.6322154	0.632199	0.6322186	0.6322187
0.5	0	1.2307661	1.230952	1.2307912	1.2307916

increases the coefficient of skin friction, mass transfer rate and decreases the heat transfer rate for both suction and injection cases. Biot number increases the friction factor, rate of heat and mass transfer.

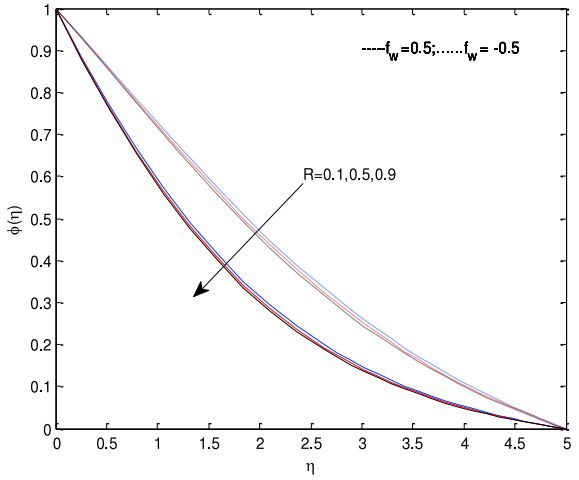

Fig. 15. Concentration profiles for different values of radiation parameter R.

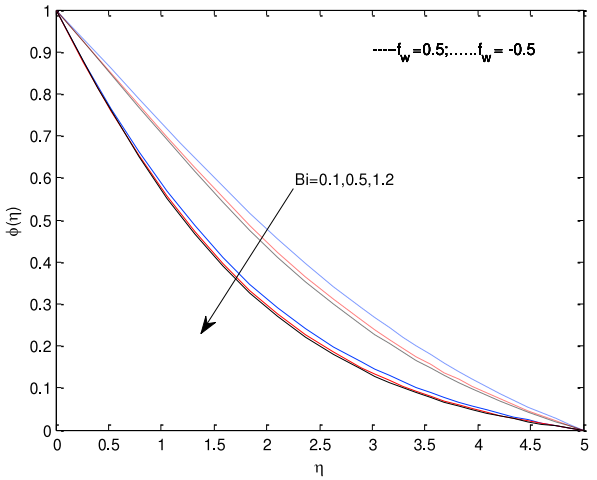

Fig. 16. Concentration profiles for different values of Biot number Bi.

Table 2
Values of $f''(0)$, $-\theta'(0)$ and $-\phi'(0)$ for different values of γ, D_f, Sr, R, Bi and f_w when Pr $=$ 0.71, $Sc = 0.6$, $\tau_T = \tau_C = 1$, $M = 2$.

Suction/ injection	γ	D_f	Sr	R	Bi	$f''(0)$	$-\theta'(0)$	$-\phi'(0)$
$f_w = 0.5$	$\pi/6$	0.3	0.2	1	0.4	−0.996652	0.262349	0.473345
	$\pi/4$	0.3	0.2	1	0.4	−1.063689	0.296702	0.458760
	$\pi/3$	0.3	0.2	1	0.4	−1.131145	0.331028	0.443636
$f_w = -0.5$	$\pi/6$	0.3	0.2	1	0.4	−0.626961	0.216991	0.261817
	$\pi/4$	0.3	0.2	1	0.4	−0.676976	0.246974	0.250243
	$\pi/3$	0.3	0.2	1	0.4	−0.726051	0.276258	0.238646
$f_w = 0.5$	$\pi/2$	1	0.2	1	0.4	−1.118960	0.324846	0.446403
	$\pi/2$	2	0.2	1	0.4	−1.377011	0.454081	0.383993
	$\pi/2$	3	0.2	1	0.4	−1.622647	0.573764	0.315286
$f_w = -0.5$	$\pi/2$	1	0.2	1	0.4	−0.717282	0.271036	0.240736

Table 2 (*continued*)

Suction/ injection	γ	D_f	Sr	R	Bi	$f''(0)$	$-\theta'(0)$	$-\phi'(0)$
	$\pi/2$	2	0.2	1	0.4	−0.893588	0.375191	0.197121
	$\pi/2$	3	0.2	1	0.4	−1.043981	0.462503	0.157087
$f_w = 0.5$	$\pi/2$	0.3	1	1	0.4	−0.915951	0.232143	0.412615
	$\pi/2$	0.3	2	1	0.4	−0.885172	0.230962	0.323503
	$\pi/2$	0.3	3	1	0.4	−0.853373	0.229715	0.236651
$f_w = -0.5$	$\pi/2$	0.3	1	1	0.4	−0.570631	0.189829	0.238047
	$\pi/2$	0.3	2	1	0.4	−0.554227	0.188424	0.198307
	$\pi/2$	0.3	3	1	0.4	−0.537735	0.186965	0.161159
$f_w = 0.5$	$\pi/2$	0.3	0.2	0.1	0.4	−1.045831	0.288475	0.463419
	$\pi/2$	0.3	0.2	0.5	0.4	−0.988038	0.257879	0.475291
	$\pi/2$	0.3	0.2	0.9	0.4	−0.947963	0.237194	0.483675
$f_w = -0.5$	$\pi/2$	0.3	0.2	0.1	0.4	−0.642050	0.224916	0.258273
	$\pi/2$	0.3	0.2	0.5	0.4	−0.609267	0.205826	0.265772
	$\pi/2$	0.3	0.2	0.9	0.4	−0.587884	0.193378	0.270678
$f_w = 0.5$	$\pi/2$	0.3	0.2	1	0.1	−1.149473	0.095241	0.475025
	$\pi/2$	0.3	0.2	1	0.5	−0.902895	0.258401	0.486982
	$\pi/2$	0.3	0.2	1	1.2	−0.776293	0.347762	0.491938
$f_w = -0.5$	$\pi/2$	0.3	0.2	1	0.1	−0.787164	0.087907	0.255005
	$\pi/2$	0.3	0.2	1	0.5	−0.552459	0.207602	0.274026
	$\pi/2$	0.3	0.2	1	1.2	−0.453942	0.261876	0.281233

4. Conclusions

This paper presents effects of aligned magnetic field, cross diffusion and radiation on steady two-dimensional flow over a stretching vertical surface. The governing partial differential equations are transformed to nonlinear ordinary differential equation by using similarity transformation and then solved by numerically by using bvp4c with Matlab package. The effects of various non-dimensional parameters on velocity, temperature, concentration profiles are discussed and presented through graphs. Also the effect of physical parameters on friction factor, Nusselt and Sherwood numbers are analyzed and presented through tables. Comparisons with existed results are presented. The findings of the numerical results are summarized as follows:

(1) Aligned angle strengthen the magneticfield parameter and it has capability to reduce the flow, friction factor, mass transfer rate and it improves rate of heat transfer.
(2) Radiation parameter helps to enhance the temperature profiles and reduce the concentration profiles, as well as heat transfer rate of the fluid. But it improves friction factor and mass transfer rate.
(3) Porosity parameter has tendency to increase the internal heat and reduces the heat transfer rate along with skin friction.
(4) Increase in soret number increases the friction factor and decreases the rate of heat and mass transfer for both suction and injection cases.
(5) Dufour number helps to enhance the heat transfer rate.
(6) Rising value in Bi increases the friction factor, Rate of heat and mass transfer.
(7) At $\gamma = \pi/2$ the aligned magneticfiled acts like transverse magneticfiled.

Acknowledgments

The authors wish to express their thanks to the very competent anonymous referees for their valuable comments and suggestions. Authors from Gulbarga University acknowledge the UGC for financial support under the UGC Dr. D.S. Kothari Post-Doctoral Fellowship Scheme (No. F. 4-2/2006 (BSR)/MA/13-14/0026).

References

[1] Prasad KV, Vajravelu K, Datti PS. The effect of variable fluid properties on the hydromagnetic flow and heat transfer over a nonlinearly stretching sheet. Int J Therm Sci 2010;49:603–10.

[2] Rashidi MM, Rostami B, Freidoonimehr N, Abbasbandy S. Free convective heat and mass transfer for MHD fluid flow over a permeable vertical stretching sheet in the presence of radiation and buoyancy effects. Ain Shams Eng J 2014;5:901–12.
[3] Mukhopadhyay Swati. MHD boundary layer flow and heat transfer over an exponentially stretching sheer embedded in a thermally stratified medium. Alex Eng J 2013;52:259–65.
[4] Pavithra GM, Gireesha BJ. Unsteady flow and heat transfer of a fluid particle suspension over an exponentially stretching sheeting. J Heat Transfer 2013;5:613–24.
[5] Zaimi K, Ishak A, Pop I. Flow past a permeable stretching/shrinking sheet in a nanofluid using two phase model. PLoS One 2014;9(11): e111743.
[6] Wang XQ, Mujumdar AS. Heat transfer characteristics of nanofluids: a review. Int J Therm Sci 2007;46:1–19.
[7] Rana P, Bhargava R. Flow and heat transfer of a nanofluid over a nonlinearly stretching sheet: a numerical study. Commun Nonlinear Sci Numer Simul 2012;17:212–26.
[8] Zaimi K, Ishak A, Pop I. Boundary layer flow and heat transfer over a non linearly permeable stretching/shrinking sheet in a nano fluid. Appl Math Comput Biol Bioinform 2014;1–8.
[9] Ahmad I, Sajid M, Awan W, Rafique M, Aziz W, Ahmed M, et al. MHD flow of a viscous fluid over an exponentially stretching sheet in a porous medium. J Appl Math 2014;1–7.
[10] Hardy FM, Ibrahim FS, Abel Gaiedz SM, Eid MR. Radiation effect on viscous flow of a nanofluid and heat transfer over a nonlinearly stretching sheet. Nanoscale Res Lett 2012;7:1–13.
[11] Bhattacharya . Heat transfer analysis in unsteady boundary layer stagnation point flow towards a shrinking/stretching sheet. Ain Shams Eng J 2013;4:259–64.
[12] Lakshminarayana PA, Murthy PVSN. Soret and dufour effect free convection heat and mass transfer from a horizontal flat plate in a Darcy porous medium. J Heat Transfer 2008;130:104504-1–104504-5.
[13] Ece MC. Free convection flow about a cone under mixed thermal boundary conditions and a magnetic field. Appl Math Model 2005;29: 1121–34.
[14] Hamad MAA, Ferdows M. Similarity solution of boundary layer stagnation-point flow towards a heated porous stretching sheet saturated with nanofluid with heat absorption/genetration and suction/blowing: A Lie group analysis. Commun Nonlinear Sci Numer Simul 2012;17: 132–40.
[15] Das SK, Choi SUS, Wenhua Yu, Pradeep T. Nanofluids science and technology. John Wiley & Sons; 2008.
[16] Buongiorno J. Convective transport in nanofluids. J Heat Transfer 2006;128:240–50.
[17] Philip J, Shima J, Raj B. Nanofluid with tunable thermal properties. Appl Phys Lett 2008;92:043108.
[18] Mohankrishna P, Sugunamma V, Sandeep N. Radiation and magneticfield effects on unsteady natural convection flow of a nanofluid past an infinite vertical plate with heat source. Chem Process Eng Res 2014;25:39–52.
[19] Sandeep N, Sugunamma V, Mohankrishna P. Effects of radiation on an unsteady natural convective flow of a EG-Nimonic 80a nanofluid past an infinite vertical plate. Adv Phys Theor Appl 2013;23:36–43.
[20] Sandeep N, Reddy AVB, Sugunamma V. Effect of radiation and chemical reaction on transient MHD free convective flow over a vertical plate through porous media. Chem Process Eng Res 2012;2:1–9.
[21] Sandeep N, Sugunamma V. Radiation and inclined magnetic field effects on unsteady hydromagnetic free convection flow past an impulsively moving vertical plate in a porous medium. J Appl Fluid Mech 2014;7(2):275–86.
[22] Khidir AA, Sibanda P. Cross-diffusion, viscous dissipation and radiation effects on an exponentially stretching surface in porous media. In: Mass. trans. advances in sustainable energy and env. oriented num. modelling. 2013. http://dx.doi.org/10.5772/55320.
[23] Makinde OD, Ogulu A. The effect of thermal radiation on the heat and mass transfer flow of a variable viscosity fluid past a vertical porous plate permeated by a transverse magneticfield. Chem Eng Commun 2008;195(12):1575–84.
[24] Makinde OD. MHD mixed-convection interaction with thermal radiation and nth order chemical reaction past a vertical porous plate embedded in a porous medium. Chem Eng Commun 2011;198(4):590–608.
[25] Seini YI, Makinde OD. MHD boundary layer due to exponentially stretching surface with radiation and chemical reaction. Math Probl Eng 2013;2013:163614. (7 pages). http://dx.doi.org/10.1155/2013/163614.
[26] Shateyi S, Makinde OD. Hydromagnetic stagnation-point flow towards a radially stretching convectively heated disk. Math Probl Eng 2013; 2013:616947. (8 pages). http://dx.doi.org/10.1155/2013/616947.
[27] Cortell R. Heat and fluid flow due to non-linearly stretching surfaces. Appl Math Comput 2011;217:7564–72.
[28] Ferdows M, Uddin MJ, Afify AA. Scaling group transformation for MHD boundary layer free convective heat and mass transfer flow past a convectively heated nonlinear radiating stretching sheet. Int J Heat Mass Transfer 2013;56:181–7.